Chemically Reacting Hydromagnetic Unsteady Flow of a Radiating Fluid Past a Vertical Plate with Constant Heat Flux

Oluwole Daniel Makinde

Institute for Advance Research in Mathematical Modelling and Computations, Cape Peninsula University of Technology, P.O. Box 652, Cape-Town 8000, South Africa

Reprint requests to O. D. M.; E-mail: makinded@cput.ac.za

Z. Naturforsch. **67a,** 239 – 247 (2012) / DOI: 10.5560/ZNA.2012-0014
Received October 11, 2011 / revised December 23, 2011

The combined effects of thermal radiation absorption and magnetic field on an unsteady chemically reacting convective flow past an impulsively started vertical plate is studied in the presence of a constant wall heat flux. Boundary layer equations are derived and the resulting approximate nonlinear partial differential equations are solved numerically using a semi-discretization finite difference technique. A parametric study of all parameters involved is conducted, and a representative set of numerical results for the velocity, temperature, and concentration profiles as well as the skin-friction parameter and Sherwood number are illustrated graphically to show typical trends of the solutions. Further validation with previous works is carried out and an excellent agreement is achieved.

Key words: Unsteady Flow; Vertical Plate; Magnetic Field; Thermal Radiation; Chemical Reaction.

1. Introduction

There is a considerable increase in the research interest in the hydromagnetic boundary layer flow with combined heat and mass transfer characteristics in the presence of buoyancy forces due to its wide range of applications in engineering, industries, and geophysics. These include magnetohydrodynamic power generators, the cooling of reactors, the solidification of alloys, convection over heat exchanger tubes, solar heating systems, thermal insulations, polymer production, manufacturing of ceramics or glassware, food processing, etc. The buoyancy forces arising from temperature and concentration differences play a significant role in several convective thermal and concentration diffusion problems whenever the flow velocity is relatively small and the temperature difference or concentration difference is relatively large [1, 2]. These buoyancy forces induce a pressure gradient in the boundary layer, which can act so as to modify the velocity, temperature, and concentration fields, and hence the rate of heat and mass transfer between the surface and the fluid [3]. In many engineering applications, it is of practical significance to consider the buoyancy effect in the study of boundary layer flows. Several researchers such as Jaiswal and Soundalgekar [4], Mahmoud and Chamkha [5], Makinde [6] have shown interest in recent years for obtaining self similar solutions of boundary layer flows with thermal and/or mass diffusion. The study of heat and mass transfer on hydromagnetic boundary layer flow of a viscous incompressible conducting fluid past an infinite vertical porous plate in presence of suction velocity was presented by Rajeswari et al. [7]. Muthucumaraswamy and Kulaivel [8] presented an analytical solution to the problem of flow past an impulsively started infinite vertical plate in the presence of heat flux and variable mass diffusion, taking into account the presence of a homogeneous chemical reaction of first order.

Moreover, many processes in engineering do occur at high temperatures and knowledge of radiation heat transfer becomes very important especially for the design of the reliable equipments. Thermal radiation effects on the boundary layer play a very important role in controlling heat transfer in polymer processing industry where the quality of the final product depends on the heat controlling factors to some extent. High temperature plasmas, cooling of nuclear reactors, liquid metal fluids, gas turbines, power generation systems, various propulsion devices for aircraft, missiles, satellites, and space vehicles are some important applications of radiative heat transfer. Makinde [9] used a superposition technique and a Rosseland diffusion flux model to study the natural convection heat and mass transfer in a gray, absorbing–emitting fluid along a porous vertical translating plate. England and Emery [10] investigated radiation effects on the laminar free convection boundary layer of an absorbing gas. Ogulu and Makinde [11] obtained a closed form solution for unsteady hydromagnetic free convection flow of a radiating fluid past a vertical plate with constant heat flux. Zueco [12] investigated the effects of radiation on free convection unsteady flow past a semi-infinite vertical plate embedded in a porous medium. A few other works of interest in this area can be found in [13 – 18].

The present paper is aimed at analyzing the effects of combined effects of radiation and magnetic field on transient flow of an electrically conducting chemically reacting, viscous, incompressible fluid past an impulsively started vertical plate with constant heat flux. The paper essentially extends the earlier results of Ogulu and Makinde [11] to include the effects of buoyancy force due to concentration gradient and Ohmic heating. Such a study has immediate applications in the chemical process engineering. A well-tested, numerically stable semi discretization finite-difference procedure known as method of line is employed to tackle the nonlinear partial differential equations governing the model problem [19]. In the following sections, the problem is formulated, solved, and discussed quantitatively.

2. Problem Formulation

Consider a two-dimensional unsteady chemically reacting flow of an incompressible, electrically conducting viscous Boussinesq fluid past an impulsively-started semi-infinite vertical plate in the presence of radiation and a transversely applied magnetic field. Here, the x'-axis is taken along the plate in the vertically upward direction, and the y'-axis is taken normal to the plate (see Fig. 1). It is assumed that a first-order chemical reaction between the diffusing species and the fluid exists. Under the above assumptions, the governing equations are based on the usual conservation laws of mass, linear momentum, energy, and mass diffusion given by Muthucumaraswamy and Kulaivel [8], England and Emery [10], Ogulu and Makinde [11], and Zueco [12]:

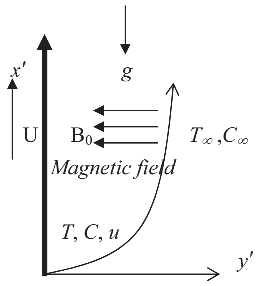

Fig. 1. Flow configuration and coordinate system.

$$\frac{\partial u'}{\partial t'} = \upsilon \frac{\partial^2 u'}{\partial y'^2} - \frac{\sigma_c B_0^2}{\rho} u' + g\beta(T - T_\infty) + g\beta_c(C - C_\infty), \tag{1}$$

$$\frac{\partial T}{\partial t'} = \frac{k}{\rho c_p}\left(\frac{\partial^2 T}{\partial y'^2}\right) + \frac{\upsilon}{c_p}\left(\frac{\partial u'}{\partial y'}\right)^2 + \frac{\sigma_c B_0^2}{\rho c_p} u'^2 - \frac{\partial q_r'}{\partial y'}, \tag{2}$$

$$\frac{\partial C}{\partial t'} = D\frac{\partial^2 C}{\partial y'^2} - \gamma(C - C_\infty), \tag{3}$$

where u' is the velocity component, T the temperature, C the concentration, t' the time, ν the kinematic coefficient of viscosity, ρ the fluid density, c_p the specific heat capacity at constant pressure, k the thermal conductivity, q_r' the radiative flux vector, σ_c the electrical conductivity, B_0 the applied magnetic field, g the acceleration due to gravity, D the chemical species mass diffusivity coefficient, γ the rate of reaction, β the coefficient of volume expansion due to temperature, β_c the coefficient of volume expansion due to concentration, and subscript '∞' denotes conditions in the free stream. For an optically thin fluid, we have [16, 18]:

$$\frac{\partial q_r'}{\partial y'} = 4\alpha^2(T - T_\infty), \tag{4}$$

where

$$\alpha^2 = \int_0^\infty \delta\lambda \frac{\partial B}{\partial T}, \tag{5}$$

and α^2 is the absorption coefficient, λ the frequency, B Planck's function, and δ the radiation absorption coefficient. The initial and boundary conditions are [8, 11]

$$t' \le 0: u' = 0,\ T = T_\infty,\ C = C_\infty \ \text{ for all } y', \tag{6}$$

$$t' > 0: \begin{cases} u' = U,\ \dfrac{\partial T}{\partial y'} = -\dfrac{q}{k},\ C = C_w \ \text{ at }\ y' = 0, \\ u' \to 0,\ T \to T_\infty,\ C \to C_\infty \ \text{ as }\ y' \to \infty, \end{cases} \tag{7}$$

where q is the constant heat flux at the plate surface and C_w is the chemical species concentration at the plate surface. We introduce the following non-dimensional quantities and parameters:

$$\begin{gathered} y = \frac{y'U}{\upsilon},\ t = \frac{t'U^2}{\upsilon},\ u = \frac{u'}{U},\ \mathrm{Pr} = \frac{\rho\upsilon c_p}{k}, \\ M^2 = \frac{\sigma B_0^2\upsilon}{\rho U^2},\ \mathrm{Gr} = \frac{g\beta\upsilon^2 q}{kU^4},\ \theta = \frac{kU(T - T_\infty)}{q\upsilon}, \\ \mathrm{Ra} = \frac{4\alpha^2\upsilon}{U^2},\ \mathrm{Ec} = \frac{kU^3}{c_p\upsilon q},\ \phi = \frac{C - C_\infty}{C_w - C_\infty}, \\ \mathrm{Sc} = \frac{\upsilon}{D},\ \mathrm{Gc} = \frac{g\beta_c\upsilon(C_w - C_\infty)}{U^3},\ h = \frac{\gamma\upsilon}{U^2}, \end{gathered} \tag{8}$$

where Pr is the Prandtl number, Gr the thermal Grashof number, Gc the solutal Grashof number, h the reaction rate parameter, M the Hartmann number, and Ra the radiation parameter. Substituting (8) into (1)–(7), we obtain

$$\frac{\partial u}{\partial t} = \frac{\partial^2 u}{\partial y^2} - M^2 u + \mathrm{Gr}\theta + \mathrm{Gc}\phi\,, \tag{9}$$

$$\frac{\partial \theta}{\partial t} = \frac{1}{\mathrm{Pr}}\frac{\partial^2 \theta}{\partial y^2} - \mathrm{Ra}\theta + \mathrm{Ec}\left(\frac{\partial u}{\partial y}\right)^2 + \mathrm{Ec}M^2u^2, \tag{10}$$

$$\frac{\partial \phi}{\partial t} = \frac{1}{\mathrm{Sc}}\frac{\partial^2 \phi}{\partial y^2} - h\phi\,. \tag{11}$$

The appropriate boundary conditions now become

$$t \le 0: u = 0,\ \theta = 0,\ \phi = 0 \ \text{ for all } y, \tag{12}$$

$$t > 0: \begin{cases} u = 1,\ \dfrac{\partial \theta}{\partial y} = -1,\ \phi = 1 \ \text{ at } y = 0, \\ u \to 0,\ \theta \to 0,\ \phi \to 0 \ \text{ as } y \to \infty. \end{cases} \tag{13}$$

Other physical quantities of interest in this problem, namely the skin friction parameter C_f and the Sherwood number Sh can be easily computed. These quantities are defined in dimensionless terms as

$$C_\mathrm{f} = -\left.\frac{\partial u}{\partial y}\right|_{y=0} \ \text{ and }\ \mathrm{Sh} = -\left.\frac{\partial \phi}{\partial y}\right|_{y=0}. \tag{14}$$

The above partial differential equation is an initial boundary value problem (IBVP) and will be solved numerically in the following section using a semi-discretization finite difference method.

3. Numerical Procedure

In order to obtain an approximate solution for the above problem, we employed a semi-discretization finite difference method known as method of lines [19]. Equations (9)–(11) together with their initial and boundary conditions (12)–(13) are transformed into a system of ordinary differential equations using finite difference for the spatial derivative. The availability of robust stiff ordinary differential equation (ODE) integrators gives an advantage to the method of lines proposed by Berzins and Ware [19]. The discretization is based on a linear Cartesian mesh and uniform grid. The spatial interval $0 \le y \le y_\infty$ is partition into N equal parts with grid size $\Delta y = 1/N$ and grid points $y_i = y_\infty i\Delta y$, $0 \le i \le N$, where y_∞ lies very well outside the momentum, energy, and concentration boundary layers. The first and second order spatial derivatives are approximated with second-order central difference. Let $u_i(t)$, $\theta_i(t)$, $\phi_i(t)$ be the approximations of $u(y_i,t)$, $\theta(y_i,t)$, and $\phi(y_i,t)$, then the semi-discrete system for the problem becomes

$$\frac{\mathrm{d}u_i}{\mathrm{d}t} = \left(\frac{u_{i+1} - 2u_i + u_{i-1}}{(\Delta y)^2}\right) - M^2u_i + \mathrm{Gr}\theta_i + \mathrm{Gc}\phi_i\,, \tag{15}$$

$$\begin{aligned} \frac{\mathrm{d}\theta_i}{\mathrm{d}t} = {} & \frac{1}{\mathrm{Pr}}\left(\frac{\theta_{i+1} - 2\theta_i + \theta_{i-1}}{(\Delta y)^2}\right) - \mathrm{Ra}\theta_i \\ & + \mathrm{Ec}\left(\frac{u_{i+1} - u_{i-1}}{2\Delta y}\right)^2 + \mathrm{Ec}M^2(u_i)^2, \end{aligned} \tag{16}$$

$$\frac{\mathrm{d}\phi_i}{\mathrm{d}t} = \frac{1}{\mathrm{Sc}}\left(\frac{\phi_{i+1} - 2\phi_i + \phi_{i-1}}{(\Delta y)^2}\right) - h\phi_i \tag{17}$$

with the initial conditions

$$u_i(0) = 0\,,\ \theta_i(0) = 0\,,\ \phi_i(0) = 0\,,\ 0 \le i \le N\,. \tag{18}$$

The equations corresponding to the first and last grid points are modified to incorporate the boundary conditions, that is,

$$\begin{gathered} u_0 = 1\,,\ \theta_2 = \theta_0 - \frac{2}{N}\,,\ \phi_0 = 1\,, \\ u_N = 0\,,\ \theta_N = 0\,,\ \phi_N = 0\,. \end{gathered} \tag{19}$$

Equation (19) is incorporated into (15)–(17) and the set of nonlinear ordinary differential equations (15)–(17) with initial conditions (18) are solved numerically by using the fourth-order Runge–Kutta integration scheme with Sc, M, Gr, Gc, Pr, Ec, h, and Ra

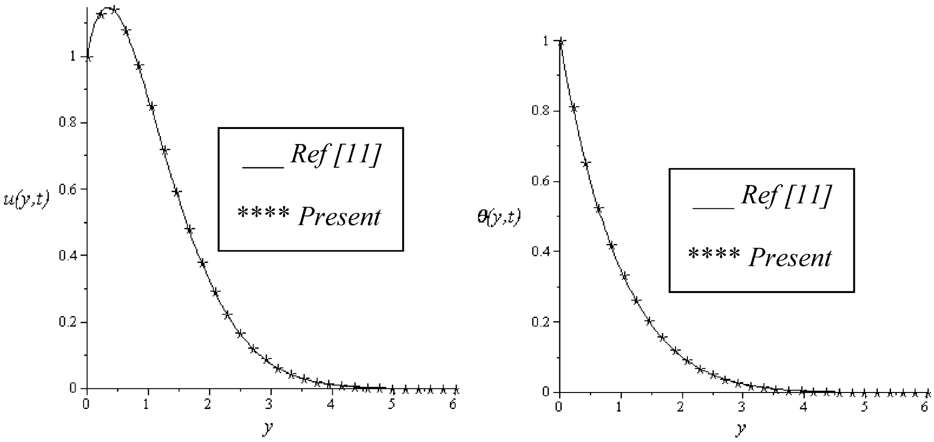

Fig. 2. Computations showing the comparison in velocity and temperature distribution with [11] when $\mathrm{Gc} = 0$, $\mathrm{Gr} = 5$, $M = \mathrm{Ra} = 1$, $\mathrm{Ec} = 0.01$, $\mathrm{Pr} = 0.71$.

as prescribed parameters. To verify the accuracy of our numerical scheme, a comparison of the computed velocity and temperature profiles is made to that of Ogulu and Makinde [11] as shown in Figure 2. Note that in this case, mass transfer and Ohmic heating are not included. From Figure 2 a perfect agreement is observed.

4. Results and Discussion

In order to illustrate the influence of the various parameters on the velocity profile (u), temperature profile (θ), concentration profile (ϕ), skin friction, and Sherwood number, numerical calculations of the solutions, obtained in the preceding section, have been carried out as shown in Tables 1 – 2 and Figures 3 – 15. To be more realistic, the value of the Prandtl number is chosen to be $\mathrm{Pr} = 0.71$ which correspond to air and $\mathrm{Sc} = 0.24$, 0.62, 0.78, 2.62, representing diffusing chemical species of most common interest in air like H_2, H_2O, NH_3, and propyl benzene, respectively. Table 1 illustrates the transient effects of the skin friction coefficient (C_f) and the mass transfer rate (Sh) at the moving plate surface when the plate is cooled by free convection current ($\mathrm{Gr} > 0$). It is interesting to note that both the skin friction and Sherwood number increase with time for a given set of parameter values until a steady state condition is achieved. In Table 2, the effects of parameter variations on the skin friction and mass transfer rate are illustrated at a fixed time ($t = 1$). The presence of a negative sign in the skin friction can be attributed to the velocity overshoot caused by buoyancy forces due to a cooling effect of the free convection current. The skin friction increases with increasing intensity of thermal and solutal Grashof numbers due to buoyancy effects while it decreases with an increase in the radiation parameter (Ra). A similar trend is observed with an increase in the magnetic field intensity (M) as well as viscous and Ohmic heating as

Table 1. Computations showing the transient effects on skin friction and Sherwood number when $\mathrm{Gr} = \mathrm{Gc} = M = \mathrm{Ra} = h = \mathrm{Ec} = 0.1$, $\mathrm{Pr} = 0.71$, $\mathrm{Sc} = 0.62$.

t	C_f	Sh
0.1	−0.02509560	0.0138512688
0.5	−0.07378508	0.0310770629
1.0	−0.12125988	0.0436456626
1.5	−0.16322726	0.0530459129
2.0	−0.20179922	0.0607765985
3.0	−0.27178847	0.0732892719

Table 2. Computations showing the effects various parameters on skin friction and Sherwood number when $t = 1$, $\mathrm{Pr} = 0.71$.

Gr	Gc	M	Ra	Sc	Ec	h	C_f	Sh
0.1	0.1	0.1	0.1	0.62	0.1	0.1	−0.1212598	0.04364566
1.0	0.1	0.1	0.1	0.62	0.1	0.1	−0.7025881	0.04364566
5.0	0.1	0.1	0.1	0.62	0.1	0.1	−3.3441388	0.04364566
0.1	1.0	0.1	0.1	0.62	0.1	0.1	−0.6791432	0.04364566
0.1	5.0	0.1	0.1	0.62	0.1	0.1	−3.1620324	0.04364566
0.1	0.1	0.5	0.1	0.62	0.1	0.1	0.01260295	0.04364566
0.1	0.1	1.0	0.1	0.62	0.1	0.1	0.37394277	0.04364566
0.1	0.1	0.1	0.5	0.62	0.1	0.1	−0.1127885	0.04364566
0.1	0.1	0.1	1.0	0.62	0.1	0.1	−0.1044142	0.04364566
0.1	0.1	0.1	0.1	0.78	0.1	0.1	−0.1180629	0.04895449
0.1	0.1	0.1	0.1	2.62	0.1	0.1	−0.1013851	0.08972136
0.1	0.1	0.1	0.1	0.62	0.2	0.1	−0.1242195	0.04364566
0.1	0.1	0.1	0.1	0.62	0.3	0.1	−0.1271730	0.04364566
0.1	0.1	0.1	0.1	0.62	0.1	0.5	−0.1179581	0.20509094
0.1	0.1	0.1	0.1	0.62	0.1	1.0	−0.1144284	0.38237721

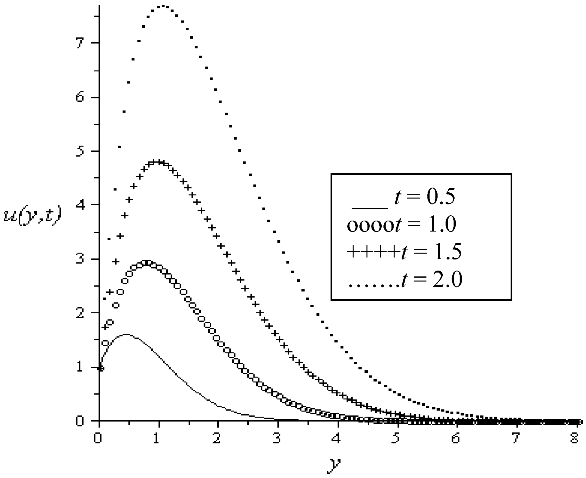

Fig. 3. Velocity profiles, $M = h = \mathrm{Ra} = \mathrm{Ec} = 0.1$, $\mathrm{Sc} = 0.62$, $\mathrm{Pr} = 0.71$, $\mathrm{Gr} = \mathrm{Gc} = 5$.

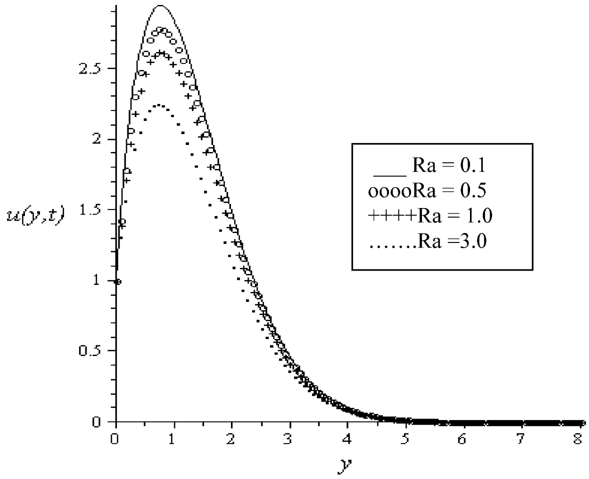

Fig. 5. Velocity profiles, $M = h = \mathrm{Ec} = 0.1$, $t = 1$, $\mathrm{Sc} = 0.62$, $\mathrm{Pr} = 0.71$, $\mathrm{Gr} = \mathrm{Gc} = 5$.

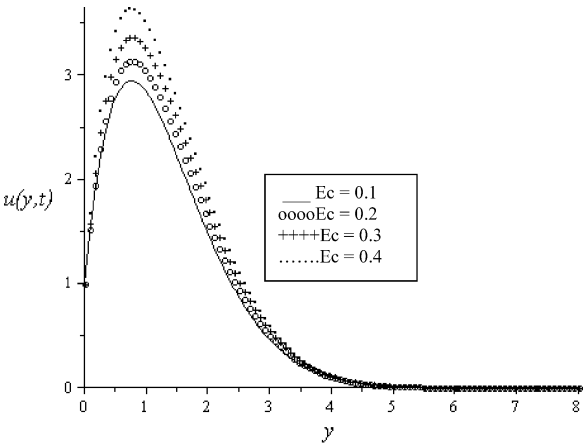

Fig. 4. Velocity profiles, $M = h = \mathrm{Ra} = 0.1$, $t = 1$, $\mathrm{Sc} = 0.62$, $\mathrm{Pr} = 0.71$, $\mathrm{Gr} = \mathrm{Gc} = 5$.

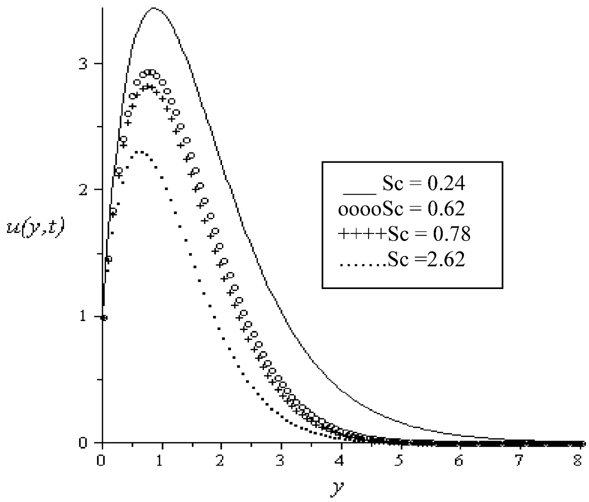

Fig. 6. Velocity profiles, $M = h = \mathrm{Ra} = \mathrm{Ec} = 0.1$, $t = 1$, $\mathrm{Pr} = 0.71$, $\mathrm{Gr} = \mathrm{Gc} = 5$.

the Ec number also increases. As the Schmidt number (Sc) and the reaction rate parameter (h) increase, the mass transfer rate increases while the skin friction decreases at the plate surface.

A. Effect of Parameter Variation on Velocity Profiles

In Figures 3 – 8, the influence of various parameters on the velocity profiles are presented. It is noteworthy that $\mathrm{Gr} = \mathrm{Gc} = 5$ correspond to strong species and thermal buoyancy forces. Generally a velocity overshoot towards the plate surface is observed and after attaining its peak value, the velocity decreases gradually to the zero far field value away from the plate. It is interesting to note that the peak value of the velocity overshoot towards the plate surface increases with time until its steady state value is achieved for a given set of parameter values as shown in Figure 3. Thus, the momentum boundary layer thickness increases in the transient flow regime. Figure 4 shows the variation of the velocity profiles with the Eckert number (Ec). The Eckert number may be interpreted as a constant measure of the heat due to viscous dissipation takes the values 0.1 and 0.4, as this will be more appropriate from the practical point of view. A slight increase in the viscous dissipation leads to an increase

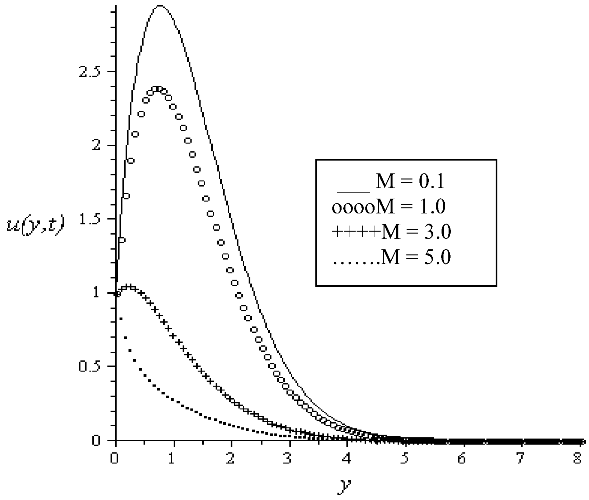

Fig. 7. Velocity profiles, $h = \mathrm{Ra} = \mathrm{Ec} = 0.1$, $t = 1$, $\mathrm{Sc} = 0.62$, $\mathrm{Pr} = 0.71$, $\mathrm{Gr} = \mathrm{Gc} = 5$.

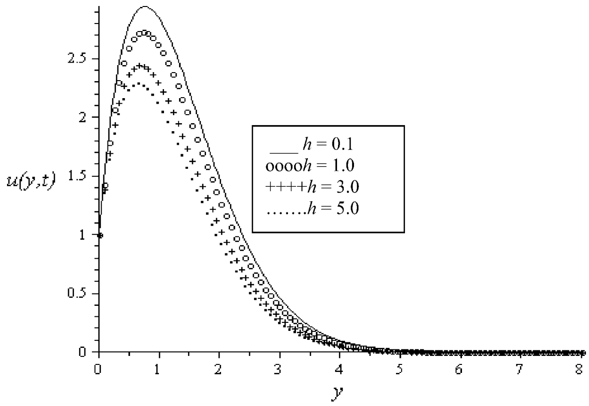

Fig. 8. Velocity profiles, $\mathrm{Ec} = M = \mathrm{Ra} = 0.1$, $t = 1$, $\mathrm{Sc} = 0.62$, $\mathrm{Pr} = 0.71$, $\mathrm{Gr} = \mathrm{Gc} = 5$.

in the velocity boundary layer thickness. Figures 5 – 8 show the effects of an increase in the parameter values of Ra, Sc, M, and h on the velocity profiles. In all cases, a decrease in the peak value of velocity overshoot which eventually lead to a decelerating flow away from the plate surface into the free stream zero value. It is also noted that with increasing values of the parameters, the velocity boundary layer thickness decreases. Hence, thermal radiation flux may affect the flow control from the surface into the boundary layer regime as illustrated in Figure 5. This is important in polymeric and other industrial flow processes since it shows that the presence of thermal radiation in the transient flow regime may affect the overall quality of the product. As the Schmidt number increases (see Fig. 6), the molecular diffusivity of the chemical species reduces leading to a decrease in the velocity profile. The effects of a transverse magnetic field on an electrically conducting fluid gives rise to a resistive-type force called the Lorentz force. This force has the tendency to slow down the fluid motion as observed in Figure 7. This result qualitatively agrees with the expectations (see [6, 7, 17]). As the reactant is consumed with increasing value of destructive reaction rate parameter (h), the reactant concentration decreases, consequently the effect of buoyancy force due to the concentration gradient diminishes leading to a decrease in the velocity profile as illustrated in Figure 8.

B. Effect of Parameter Variation on Temperature Profiles

Figures 9 – 12 illustrate the temperature field against spanwise coordinate y. The fluid temperature is highest at the plate surface and decreases exponentially to the free stream zero value far away from the plate satisfying the boundary condition. In Figure 9, we observed an increase in both the plate surface temperature and the fluid temperature within the transient flow regime as the values of t increases for a given set of parameter values until a steady state is achieved. Consequently, one can conclude that the thermal boundary layer thickness increases within the transient flow regime. A similar trend is observed in Figure 10 with increasing magnetic field intensity parameter (M) which invariably contributes to the presence of Ohmic

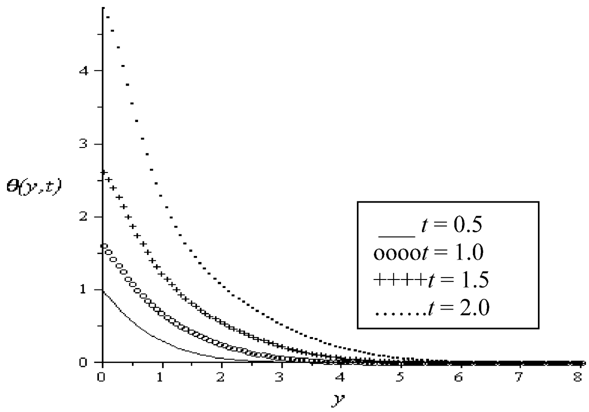

Fig. 9. Temperature profiles, $M = h = \mathrm{Ra} = \mathrm{Ec} = 0.1$, $\mathrm{Sc} = 0.62$, $\mathrm{Pr} = 0.71$, $\mathrm{Gr} = \mathrm{Gc} = 5$.

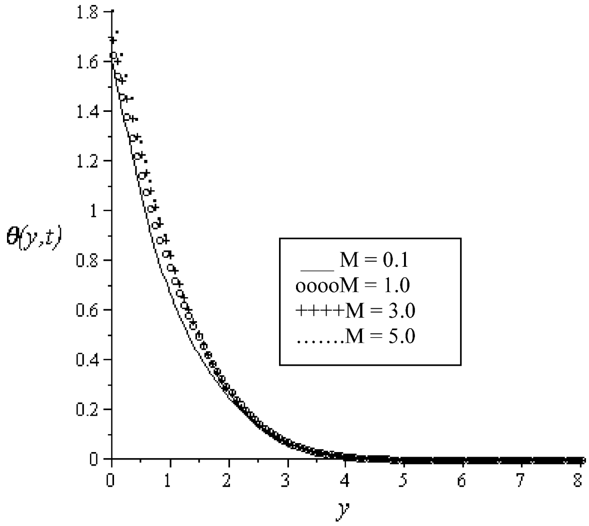

Fig. 10. Temperature profiles, $h = \mathrm{Ra} = \mathrm{Ec} = 0.1$, $t = 1$, $\mathrm{Sc} = 0.62$, $\mathrm{Pr} = 0.71$, $\mathrm{Gr} = \mathrm{Gc} = 5$.

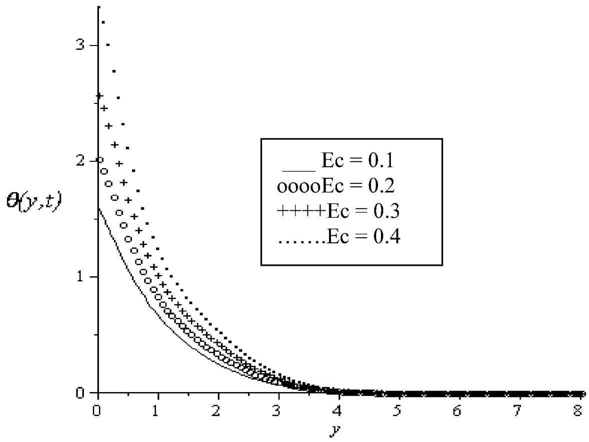

Fig. 11. Temperature profiles, $M = h = \mathrm{Ra} = 0.1$, $t = 1$, $\mathrm{Sc} = 0.62$, $\mathrm{Pr} = 0.71$, $\mathrm{Gr} = \mathrm{Gc} = 5$.

heating, leading to an increase in the fluid temperature and thermal boundary layer thickness. Figure 11 depicts the influence of the Eckert number on the thermal boundary layer. As more heat is generated within the fluid due to viscous dissipation effects, the fluid temperature increases leading to an increase in the plate surface temperature. The thermal boundary layer thickness also increases with an increase in Eckert number. An increase in the thermal radiation (Ra) causes a decrease in the fluid temperature within the boundary layer and consequently the thermal boundary layer decreases as shown in Figure 12.

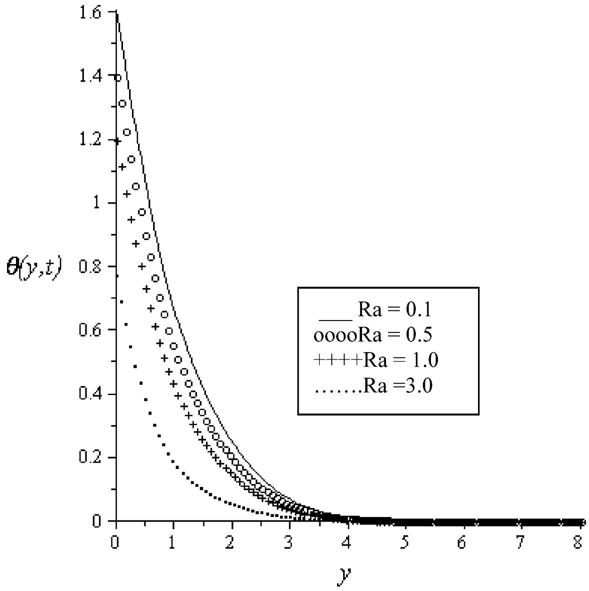

Fig. 12. Temperature profiles, $M = h = \mathrm{Ec} = 0.1$, $t = 1$, $\mathrm{Sc} = 0.62$, $\mathrm{Pr} = 0.71$, $\mathrm{Gr} = \mathrm{Gc} = 5$.

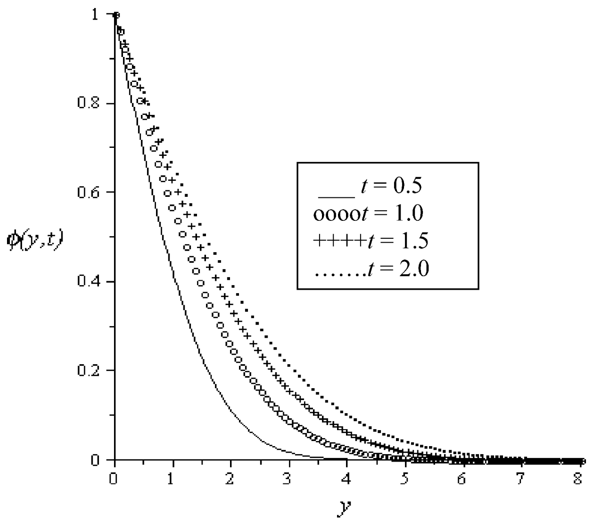

Fig. 13. Concentration profiles, $M = h = \mathrm{Ra} = \mathrm{Ec} = 0.1$, $\mathrm{Sc} = 0.62$, $\mathrm{Pr} = 0.71$, $\mathrm{Gr} = \mathrm{Gc} = 5$.

C. Effect of Parameter Variation on Concentration Profiles

Figures 13 – 15 present typical profiles for chemical species concentration against spanwise coordinate y. The chemical species concentration is highest at the plate surface and decreases exponentially to the free

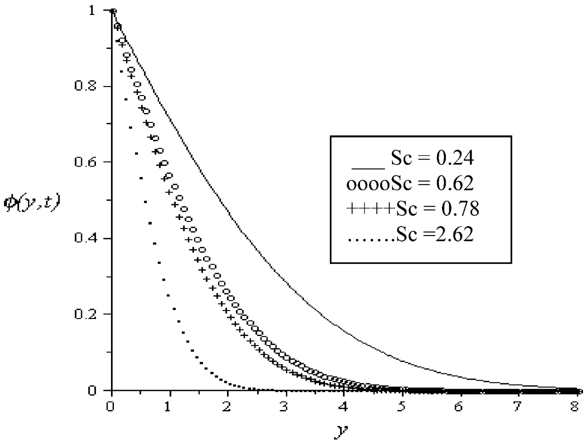

Fig. 14. Concentration profiles, $M = h = \mathrm{Ra} = \mathrm{Ec} = 0.1$, $t = 1$, $\mathrm{Pr} = 0.71$, $\mathrm{Gr} = \mathrm{Gc} = 5$.

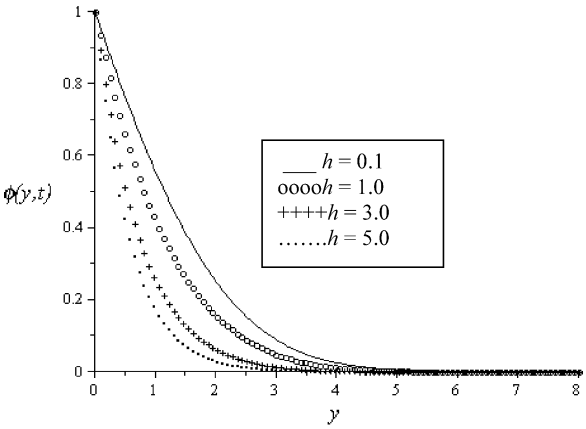

Fig. 15. Concentration profiles, $\mathrm{Ec} = M = \mathrm{Ra} = 0.1$, $t = 1$, $\mathrm{Sc} = 0.62$, $\mathrm{Pr} = 0.71$, $\mathrm{Gr} = \mathrm{Gc} = 5$.

stream zero value far away from the plate. It is observed in Figure 13 that the chemical species concentration increases in the transient flow regime with increasing value of t at a given set of parameter values until a steady state is achieved. This clearly shows that the concentration boundary layer thickness increases within the transient flow regime until steady state is achieved. An increase in Schmidt number (Sc) as shown in Figure 14 decreases the concentration boundary layer and this can be attributed to the fact that as Sc increases the molecular mass diffusivity of the reacting chemical specie decreases, consequently the species concentration decreases within the boundary layer region. A similar trend is observed in Figure 15 with increasing destructive reaction rate (h). Since as h increases, the reactant is consumed, leading to a decrease in the chemical species concentration within the boundary layer region.

5. Conclusions

An analysis is performed to study the combined effects of magnetic field and thermal radiation on a conducting chemically reacting transient flow past an impulsively started moving vertical plate with viscous dissipation, Ohmic heating and constant heat flux. The nonlinear dimensionless governing partial differential equations are solved numerically using a semi-discretization method known as method of line. It is observed that the fluid velocity, temperature, and concentration increase within the transient flow regime for a given set of parameter values until a steady state is achieved. Both the fluid velocity and temperature decrease as the radiation parameter (Ra) increases but it increases with an increase of the viscous heating parameter (Ec). The presence of thermal and solutal Grashof numbers (Gr, Gc) causes an overshoot in the velocity profile towards the plate surface as a result of buoyancy forces. Moreover, the fluid velocity decreases while the temperature increases with an increase in the magnetic field parameter (M). The concentration boundary layer thickness decreases with increasing values of reaction rate parameter (h) and Schmidt number (Sc). It is found that both the skin friction and the mass transfer rate increase within the transient flow regime.

Acknowledgements

The author would like to thank the National Research Foundation of South Africa Thuthuka programme for financial support.

[1] Y. A. Guloyan, Glass Ceram. **60**, 233 (2003).
[2] H. Liu and K. E. Thompson, Comput. Chem. Eng. **26**, 1595 (2002).
[3] J. Qi and R. F. Savinell, J. Appl. Electrochem. **23**, 873 (1993).
[4] B. S. Jaiswal and V. M. Soundalgekar, Heat Mass Transfer **37**, 125 (2001).
[5] A. A. Mahmoud and A. J. Chamkha, Int. J. Chem. React. Eng. **8**, 1 (2010).

[6] O. D. Makinde, Int. J. Numer. Method. H. **19**, 546 (2009).

[7] R. Rajeswari, B. Jothiram, and V. K. Nelson, Appl. Math. Sci. **3**, 2469 (2009).

[8] R. Muthucumaraswamy and T. Kulaivel, Forsch. Ingenieurwes. **68**, 101 (2003).

[9] O. D. Makinde, Int. Commun. Heat Mass **32**, 1411 (2005).

[10] W. G. England and A. F. Emery, J. Heat Transf. **91**, 37 (1969).

[11] A. Ogulu and O. D. Makinde, Chem. Eng. Commun. **196**, 454 (2009).

[12] J. Zueco, Commun. Numer. Meth. Eng. **24**, 1093 (2008).

[13] A. J. Chamkha, J. Heat Transf. **119**, 89 (1997).

[14] A. Y. Bakier, Int. Commun. Heat Mass **28**, 119 (2001).

[15] L. K. Yang, Int. Commun. Heat Mass **19**, 249 (1992).

[16] A. Raptis and C. Perdikis, Int. J. Appl. Mech. Eng. **8**, 131 (2003).

[17] O. D. Makinde and T. Chinyoka, Commun. Nonlinear Sci. **15**, 3919 (2010).

[18] M. Q. Brewster, Thermal Radiative Transfer Properties, John Wiley and Sons, Chichester 1972.

[19] M. Berzins and J. M. Ware, Appl. Numer. Math. **20**, 83 (1996).